

Measurement of voltage-dependent electronic transport across amine-linked single-molecular-wire junctions

J R Widawsky^{1,2}, M Kamenetska^{1,2}, J Klare^{2,3}, C Nuckolls^{2,3},
M L Steigerwald³, M S Hybertsen⁴ and L Venkataraman^{1,2}

¹ Department of Applied Physics and Applied Mathematics, Columbia University, NY 10027, USA

² Center for Electron Transport in Molecular Nanostructures, Columbia University, NY 10027, USA

³ Department of Chemistry, Columbia University, NY 10027, USA

⁴ Center for Functional Nanomaterials, Brookhaven National Labs, Upton, NY 11973, USA

Received 15 June 2009, in final form 17 August 2009

Published 2 October 2009

Online at stacks.iop.org/Nano/20/434009

Abstract

We measure the conductance and current–voltage characteristics of two amine-terminated molecular wires—4,4′-diaminostilbene and bis-(4-aminophenyl)acetylene—by breaking Au point contacts in a molecular solution at room temperature. Histograms compiled from thousands of measurements show a slight increase in the molecular junction conductance (I/V) as the bias is increased to nearly 450 mV. Comparatively, similar conductance measurements made with 1,6-diaminohexane, a saturated molecule, demonstrate almost no bias dependence. We also present a new technique to measure a statistically defined current–voltage ($I-V$) curve. Application to all three molecules shows that 4,4′-diaminostilbene exhibits the largest increase in differential conductance as a function of applied bias. This indicates that the predominant transport channel for 4,4′-diaminostilbene (the highest occupied molecular orbital) is closer to the Fermi level of the metal than that of the other molecules, consistent with the trends observed in the molecular ionization potential. We find that junctions constructed with the conjugated molecules show greater noise in individual junctions and less structural stability, on average, at biases greater than 450 mV. In contrast, junctions formed with the alkane can sustain a bias of up to 900 mV. This significantly affects the statistically averaged $I-V$ characteristic measured for the conjugated molecules at higher bias.

1. Introduction

Understanding charge transport across metal–molecule–metal junctions could lead to the development of nanoscale devices with functionality that can be tuned chemically [1]. It is thus important to fully understand the mechanisms behind charge transport across single-molecule junctions. In the last decade, the characterization of the electronic properties of single-molecule junctions has been studied extensively by different methods [16, 12, 10, 17, 21, 3, 4, 20, 11, 2]. These have focused both on measuring the low bias conductance of a molecular junction as well as the current–voltage characteristics under applied voltages up to the 1 V range or larger. However, in practice, it is often hard to confirm that a single molecule is actually bridging the metal electrodes and

to assess the structural stability of the molecular conformation while the current is measured as a function of voltage. Furthermore, a detailed understanding of these properties requires the measurement of a statistically significant number of junctions. As a result, experiments that directly correlate molecular structure and current–voltage characteristics remain challenging.

Here, we investigate the conductances of two short amine-linked molecular wires: 4,4′-diamino-stilbene (**1**), which consists of two benzene rings with a vinyl bridge ($C=C$), and bis-(4-aminophenyl)acetylene (**2**), which is similar but with an ethynyl bridge ($C\equiv C$), and compare them to that of 1,6-hexanediamine (**3**). The molecular structures are illustrated in figure 1(A). These molecules bind to gold metal electrodes through an electronically selective donor–acceptor

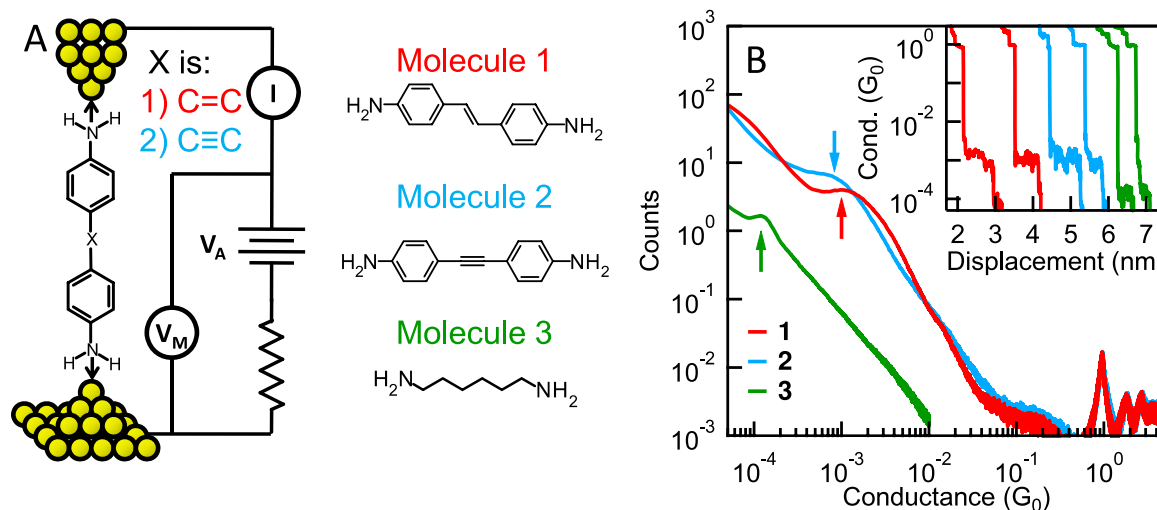


Figure 1. (A) Schematic of experimental set-up: V_A is the applied bias voltage, I is the measured current and V_M is the voltage measured across the junction. The ~ 100 k Ω series resistor is also shown. Structures of all three molecules are also shown. The N–N length of these molecules are about 1.2 nm, 1.3 nm and 0.9 nm for **1**, **2** and **3**, respectively. The molecules bind to the gold leads through the lone pair of the amines, represented here by arrows. (B) Normalized conductance histograms for all three molecules measured with a bias $V_M = 45$ mV and a 1 mM solution of the molecules in 1,2,4-trichlorobenzene. A linear bin size of $10^{-5}G_0$ is used for **1** and **2** (showing molecular peak and conductance quantum peaks) and a bin size of $10^{-6}G_0$ is used for **3**. The peaks, determined using Lorentzian fits (or Lorentzian fit with background subtraction for **2**), are marked with arrows. Inset: sample measured traces for each of the three molecules showing the molecular conductance steps. All traces except for the extreme left trace have been offset horizontally to the right for clarity.

bond formed between the N-lone pair on the terminal amine link groups and an under-coordinated gold atom [18]. We present a new measurement technique to probe the single-molecule junction differential conductance as a function of applied bias voltage. We find that, at a bias of about 400 mV, the differential conductance of **1** increases the most, the differential conductance of **2** increase modestly while **3** shows almost no bias dependence. Since transport in these amine-linked molecules is mediated through the highest occupied molecular orbital (HOMO) [19], these results indicate that the HOMO for **1** is closest to the metal Fermi level. Furthermore, we find that molecular junctions of **1** and **2** become unstable at a higher bias, while **3** can sustain a bias of up to about 900 mV. This suggests that the amine–Au bond can sustain a high bias. However, the partial charging of the resonant level supporting transport in steady state at higher bias, as suggested by the proximity of the HOMO to the Au Fermi level in **1** and **2**, acts to weaken the donor–acceptor bond.

2. Experimental method

We form single-molecule junctions by breaking a gold point contact in a solution of the molecules [21] and measure the conductance while pulling the junction apart at a constant speed of 16 nm s^{-1} . Molecule **1** was obtained from Astatech (97% purity), molecule **2** was synthesized as described earlier [5] and molecule **3** was obtained from Sigma-Aldrich (>99% purity). Details of our experimental set-up have been described previously [5]. Briefly, we use a home-built modified scanning tunneling microscope (STM), designed with only z -axis mobility. The STM tip is a high-purity (5N) gold wire (Alfa Aesar), 0.025 inches in diameter, cut on an angle to be sharp. The STM substrate consists of 100 nm of gold

thermally evaporated onto mica, which was cleaned under UV/ozone prior to use. The measurements are carried out at room temperature, in ambient conditions. We measure the current (I) through the tip–substrate junction using a current amplifier. In the measurements described here, we place a 100 k Ω resistor in series with our tip–substrate junction to limit the voltage drop across the junction when its resistance is very low (figure 1(A)). A bias (V_A) is applied across the junction and series resistor. We measure the bias (V_M) across the tip–substrate junction and determine the conductance ($G = I/V_M$) by dividing the measured current with the measured voltage.

For single-molecule-junction current–voltage measurements (I – V), the STM tip is brought into contact with the Au substrate until a conductance of greater than a few G_0 is obtained at an applied bias of about 50 mV. The tip is then withdrawn by 2.4 nm at 16 nm s^{-1} . This distance is chosen to ensure that the gold point contact is broken by the end of this elongation, a prerequisite for forming a molecular junction. At this point, the tip–substrate distance is held constant for about 150 ms. During this ‘hold’ period, the V_A is ramped sinusoidally for one period and the current is measured. At the end of this ramp, V_A is set to 50 mV once again and the tip is withdrawn an additional 2.4 nm to fully break the junction.

3. Results and discussions

We first measure the conductance of the three molecules in separate experiments at a low bias ($V_M \sim 45$ mV) from ~ 1 mM solutions of the compounds in 1,2,4-trichlorobenzene (Sigma-Aldrich, >99% purity). The inset of figure 1(B) shows sample conductance traces measured with each of the three molecules, showing steps at integer multiples of $G_0 = 2e^2/h = 77.5$ μS , the quantum of conductance, and at

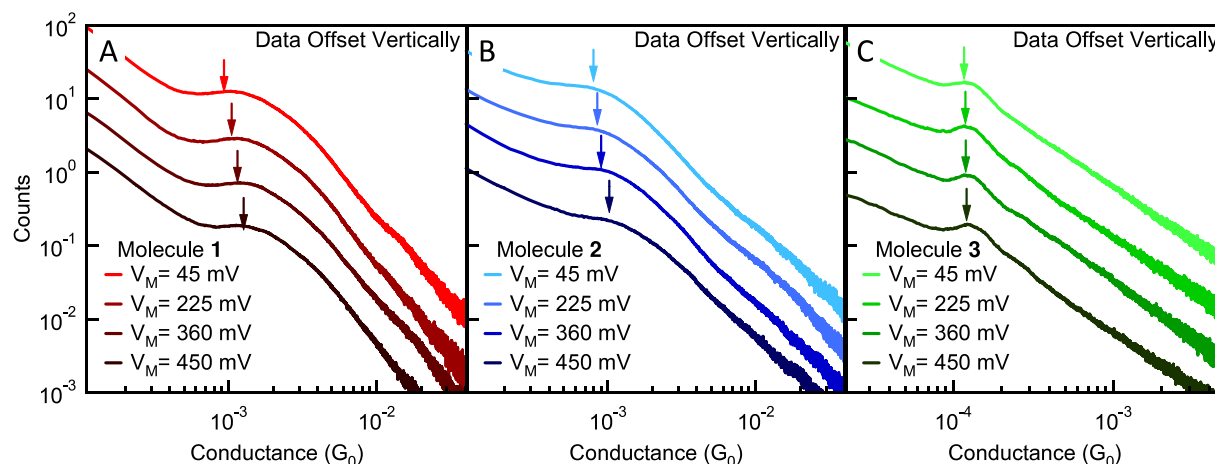


Figure 2. Linearly binned normalized conductance histograms constructed from over 5000 traces without data selection for **1**, **2** and **3** ((A), (B) and (C), respectively) measured at four different bias voltages, V_M . The peak locations are tracked by the arrows. Note: the histograms have been offset vertically for clarity.

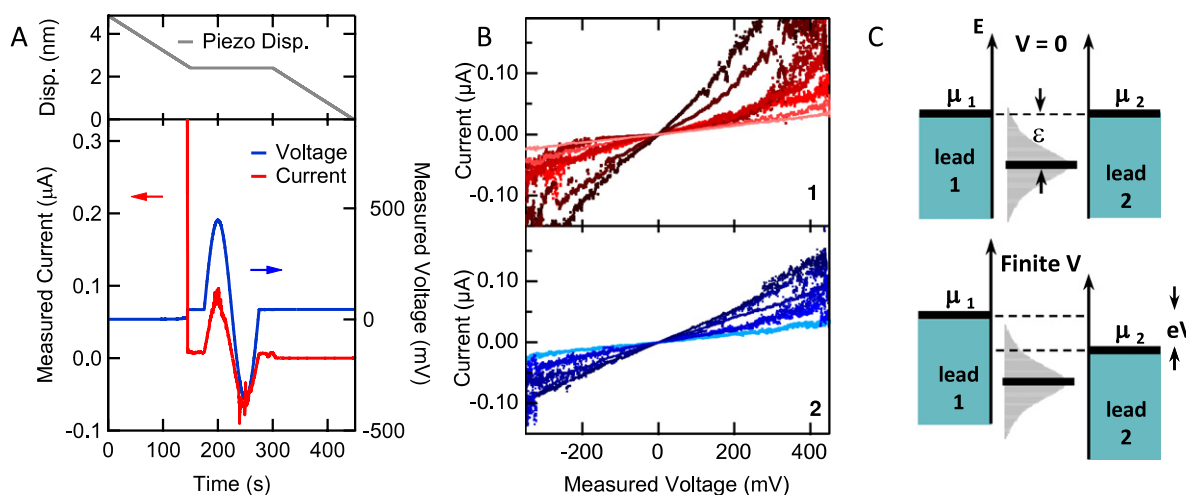


Figure 3. (A) Sample trace measured during a voltage sweep for molecule **1**. The piezodisplacement (gray line) is shown in the upper panel. The measured current (red, left axis) and voltage (blue, right axis) are shown in the bottom panel. Note that the voltage is very low when the junction conductance is low due to the series resistor. (B) Multiple sample current–voltage traces for molecules **1** (upper panel) and **2** (lower panel). These traces are obtained from the middle section of the voltage sweep, with V_M starting at +450 mV and ending at –350 mV and are chosen to illustrate the variety in measured traces. (C) Schematic level alignment diagram for two different biases showing the change in charge transfer (extent of gray shaded region within the bias window) between the molecule and metal at a large applied bias.

a molecule-dependent value below G_0 . In figure 1(B), we show conductance histograms constructed from thousands of consecutively measured traces with each molecule at $V_M \sim 45$ mV. A histogram measured in the solvent alone has no features over this conductance range. By using Lorentzian fits to the peaks (or a Lorentzian fit with a power-law background for **2**), we are able to extract the most-probable conductance value for each molecule. We see a peak centered at about $1.0 \times 10^{-3} G_0$, $0.8 \times 10^{-3} G_0$ and $1.2 \times 10^{-4} G_0$ for molecules **1**, **2** and **3**, respectively, consistent with previous results [5]. For **2**, we need to subtract a power-law background because the peak is broad, probably due to the soft rotation barrier about the $\text{C}\equiv\text{C}$ bridge [9, 5]. To determine the bias dependence of these conductance histograms, we measure conductance traces at different constant biases. For each molecule, four different biases ranging from $V_M \sim 45$ to 450 mV were

used and between five and ten thousand conductance (I/V_M) traces were compiled for each molecule at each bias to give the conductance histograms. Results of these bias-dependent measurements are shown in figure 2, where the peak of the conductance histogram, indicated by the arrows, shifts to higher conductance with increasing bias for **1** and **2**, as opposed to **3** where there is almost no change in the peak position.

These measurements give average conductance (I/V) versus applied bias; to measure the differential conductance (dI/dV) of these molecules as a function of applied bias, we first construct a statistically significant I – V curve for each molecule as follows. We measure thousands of I – V curves on single-molecule junctions while holding the relative tip-sample displacement fixed as described in section 2. A sample measured trace for molecule **1** is shown in figure 3(A) to

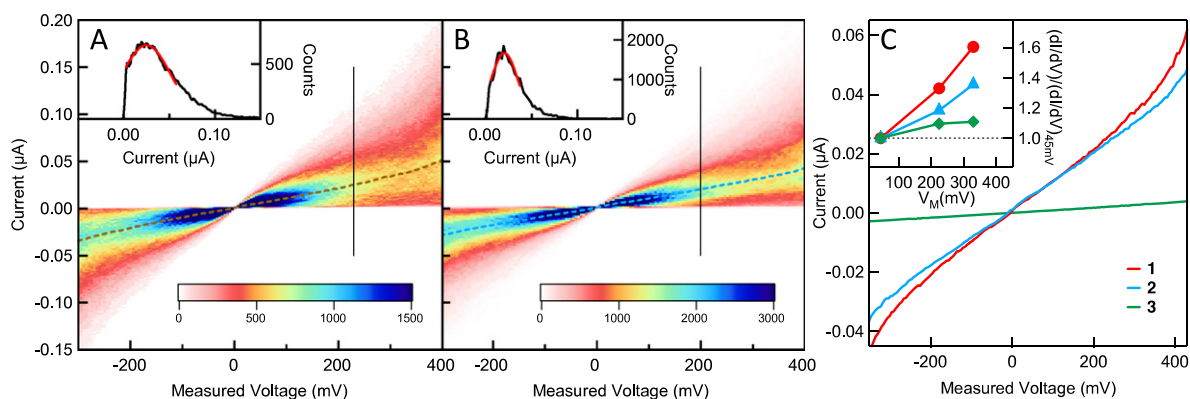


Figure 4. (A) and (B) Two-dimensional current–voltage histogram for **1** and **2** made from about 4500 and 6000 individual $I-V_M$ traces, respectively. The current bin size is 0.5 nA and the voltage bin size is 5 mV. A vertical cross section (black line) is displayed in the inset. The upper part is fitted with a Gaussian (red curve) in order to extract the peak location. (C) $I-V$ curves for **1** (red), **2** (blue) and **3** (green) determined from the peak locations of the cross sections at all voltage bins, like those shown in the insets of (A) and (B). The curves represent the most frequently measured current as a function of bias voltage. Inset: relative differential conductance (dI/dV) for **1**, **2** and **3** normalized to the respective differential conductance values at $V_M = 45$ mV. These are obtained from the slopes of the linear fits to the IV curves in a small voltage interval about each voltage.

illustrate the method, showing the piezo displacement, the measured current (I) and measured bias (V_M) when a bias ramp of about ± 450 mV is applied. Thousands of such $I-V_M$ traces were measured with each molecule. We further analyzed only those traces for which the conductance just before and just after the voltage ramp was within the peak seen in the respective conductance histograms shown in figure 1(B). These were selected using an automated algorithm. We found that about 15–25% of the measured traces had a molecule bridging the tip and the substrate during the ‘hold’ section for molecules **1** and **2**, although about 95% of our conductance versus displacement traces had a molecule. Thus some junctions broke within the initial 2.4 nm extension, some did not break until after the 150 ms ‘hold’ section and some junctions did not sustain the bias ramp, bringing down the total number of successful $I-V_M$ measurements. In our measurements with molecule **3**, only 5% of the measurements resulted in successful $I-V_M$ traces, even though about 85% of the traces had a molecule bridging the tip and substrate. In figure 3(B) we show sample $I-V_M$ traces for molecules **1** and **2**, where we can see that the current increases through the junction with increasing bias. These $I-V_M$ curves were chosen to illustrate the variety in measured $I-V_M$ curves. We find that $I-V$ traces for molecule **1** are much noisier at high bias than those for molecule **2** or **3**. A possible reason for this will be discussed below.

The selected $I-V_M$ data were then used to construct a two-dimensional histogram of current versus voltage. Such histograms, obtained for **1** from about 4500 $I-V_M$ traces and for **2** from about 6000 traces, are shown in figures 4(A) and (B). An analogous histogram was also constructed for **3** but is not shown here. We fit Gaussians to vertical sections at each voltage bin of the histogram (as demonstrated in the insets of figures 4(A) and (B)) to track the peak in the current distribution as a function of voltage. These correspond to the most frequently measured current at each bias voltage for all molecular junctions. The peak position is traced with the dotted curves shown in figures 4(A) and (B). The resulting

$I-V_M$ measurements of **1**, **2** and **3** are shown in figure 4(C) (solid lines). We determine the differential conductance for all three molecules by taking the slope of these $I-V_M$ curves at a few fixed bias values. The inset of figure 4(C) shows the differential conductance (dI/dV) normalized to its value at 45 mV ($dI/dV_{45\text{ mV}}$). We can see that the dI/dV of **1** shows the largest increase with applied bias, that of **2** shows a small increase while **3** shows almost no bias dependence.

Two factors control the conductance of these single-molecule junctions in the non-resonant tunneling regime: (1) the position of the dominant transport channel, the HOMO [19, 15, 8, 14], relative to the metal Fermi level and (2) the coupling of the HOMO level to the metal, resulting in a level broadening (figure 3(C)). Both could be different for different molecules. The net effect of these two factors determines the tunnel coupling across the junction. Using a density functional theory (DFT)-based approach [6, 13], we have previously shown that the trends in the tunnel coupling can be determined by modeling the electronic structure of a single under-coordinated Au atom bonded to each side of the junction [5]. In particular, the tunnel coupling for **1** is found to be about 20% larger than that for **2**. The position of the HOMO relative to the Fermi level can only be determined from a full transmission calculation including corrections for correlation effects beyond DFT [15]. Such calculations are beyond the scope of this paper. However, we have previously measured the effect of substituents on the conductance of benzenediamine [19]. Electron-withdrawing substituents reduced conductance while electron-donating substituents increased conductance. Electron-withdrawing groups lower the molecular orbital energies (increase ϵ in figure 3(C)) and the opposite for electron-donating groups. The conductance results are only consistent with the HOMO being the closest to the Fermi energy and mediating the tunneling conductance. These trends were understood using a vertical ionization potential calculation for the substituted species. Subsequent full transmission calculations for benzenediamine

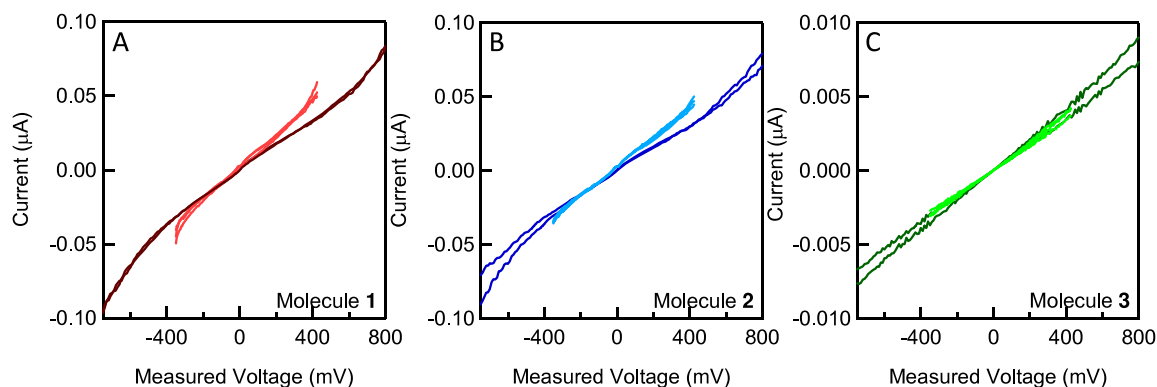


Figure 5. Average I – V curves determined from 2D I – V_M histograms using a small ramp (± 450 mV) or large ramp (± 900 mV) for all three molecules. Each averaged I – V curve is determined from one tip/sample pair and two or three such datasets are superposed for each molecule and ramp value. Variations in the I – V curves from the small and large bias ramps are larger for **1** and **2** than the variations.

confirmed that the HOMO was the sole channel responsible for low bias conductance, with an estimated separation $\varepsilon \approx 3$ eV, including corrections to DFT orbital energies, and a half-width of about 0.5 eV [15, 14]. Calculations for amine-linked alkanes show an even larger separation [8].

For the three molecules under study here, we calculated the vertical ionization potential with a triple zeta basis (including polarization and diffuse functions) and found them to be 6.11 eV, 6.25 eV and 7.67 eV for **1**, **2** and **3**, respectively. For reference, the calculated value for benzenediamine is 6.83 eV. The DFT calculations moderately underestimate diamine ionization potentials [19], as also observed for other aromatics [7], but represent the trends. The calculations clearly suggest that the molecular wires (**1** and **2**) should have the HOMO level closer to the electrode Fermi energy than benzenediamine, but not by enough to reach the resonant tunneling regime for the bias ranges under study here. However, as the sketch in figure 3(C) illustrates, proximity to the resonance can lead to enhanced differential conductance. The calculated ionization potentials suggest a larger increase in the differential conductance of **1** compared with **2** at elevated bias. However, the magnitude of the effect observed at 400 mV bias suggests that a more complete transmission calculation will be required for full understanding. On the other hand, the relatively constant differential conductance for the alkane **3** with bias is consistent with the HOMO-derived resonance remaining substantially outside the bias window.

To probe this further, we performed similar I – V measurements by applying a bias ramp of about ± 900 mV to all three molecules. Two-dimensional histograms of the selected I – V_M measurements were created and the most frequently measured current versus voltage curves were determined for all three molecules, as described in detail above. We found that the fraction of traces where molecule **1** or **2** bridged the tip–substrate gap was about 10% with the ± 900 mV ramp compared with 15%–25% for the ± 450 mV ramp. This implies that fewer junctions could sustain a ± 900 mV applied bias. For molecule **3** there was no significant difference in the trapping probability with the two different ramps. In figure 5, we compare I – V_M curves for all three molecules with both bias ramps. We see that the I – V_M

curves for **1** and **2** have a lower average conductance (I/V_M) with the ± 900 mV ramp when compared with the ± 450 mV ramp. Since these measurements represent the most frequently measured current at each voltage, they imply that, for **1** and **2**, the types of junctions measured differ between the two ramps; junctions with a higher average conductance cannot sustain a bias of about 900 mV. In contrast, for **3**, the I – V curves are almost identical. This suggests a correlation between the conductance of an individual junction and stability of the junction under higher applied bias. One physical explanation for such a correlation would be variations in the proximity of the HOMO to the electrode Fermi energy. Larger conductance corresponds to larger overlap of the HOMO-derived transmission resonance to the electrode Fermi energy, resulting in an increased charge transfer from the molecular HOMO to the metal (figure 3(C)). As the applied bias is increased, the portion of the resonance in the bias window increases, resulting in more charge transfer. Thus for **1** and **2**, which have a smaller HOMO–LUMO gap, we expect a larger charge transfer between the electrode and the molecules, while for **3**, which has a very large HOMO–LUMO gap, we do not expect a significant change in this charge transfer. There are two donor–acceptor bonds that hold the diamine in place between the emerging Au tips; we hypothesize that this charge redistribution, while it may strengthen one of these bonds, must weaken the other. This weakening of one bond could result in noisier I – V curves, as we find experimentally. Furthermore, the cleavage of this weaker link destroys the molecular junction. The extent to which this bias-dependent charge transfer strongly correlates with conductance could account for the differences observed between low and high applied bias range in both noise level in individual I – V characteristics of individual junctions and the changes in the averaged I – V curves. Molecule **1** has the highest conductance, and thus a molecular level closest to the Fermi level when comparing these three molecules. We expect a greater charge transfer in molecular junctions with **1**. Experimentally, this would result in noisier I – V curves due to a decrease in the N–Au bond strength, as well as a reduced ability to sustain higher biases (decreasing number of successful I – V measurements.) Molecule **2** would show a similar trend, though the extent

of charge transfer would be smaller as it is less conducting, and therefore has a HOMO level that is not as close to the Fermi level. For **3**, which has a very large HOMO–LUMO gap, we do not expect a significant change in transfer when comparing an applied bias of 0.4 or 0.8 V, consistent with the experiment. We also note that, while the N-lone pair on the amine link group remains highly localized for the alkanes, it is significantly coupled to the π electron HOMO for **1** and **2**, further supporting a connection between charge removal from the HOMO and bond strength in these cases.

4. Conclusions

We have presented a new technique to measure statistically averaged current–voltage characteristics of single-molecule junctions and have applied this technique to measure the differential conductance of 4,4'-diaminostilbene (**1**) and bis-(4-aminophenyl)acetylene (**2**) single-molecule junctions as a function of bias voltage. We find that both molecules show an increase in differential conductance as a function of applied bias, in contrast to measurements of 1,6-diaminohexane (**3**). This is consistent with trends in the ionization potential for the three molecules. We further find that junctions with **1** and **2** show significant increases in noise and reductions in stability at applied biases above about 450 mV, while junctions with **3** remain stable to a bias voltage of 900 mV. This significantly affects the statistically averaged I – V characteristics at high applied bias for **1** and **2**.

Acknowledgments

This work was supported in part by the NSF-NSEC (award no. CHE-0641523), by NYSTAR, the American Chemical Society under the Petroleum Research Fund and Columbia University RISE award. This work was supported in part by the DOE (DE-AC02-98CH10886). LV thanks NSF Career Award CHE-0744185 and the David and Lucille Packard Foundation.

References

- [1] Aviram A and Ratner M A 1974 Molecular rectifiers *Chem. Phys. Lett.* **29** 277–83
- [2] Blum A S, Kushmerick J G, Pollack S K, Yang J C, Moore M, Naciri J, Shashidhar R and Ratna B R 2004 Charge transport and scaling in molecular wires *J. Phys. Chem. B* **108** 18124–8
- [3] Dadosh T, Gordin Y, Krahn R, Khivrich I, Mahalu D, Frydman V, Sperling J, Yacoby A and Bar-Joseph I 2005 Measurement of the conductance of single conjugated molecules *Nature* **436** 677–80
- [4] Emanuel L, Heiko B W and Heike R 2007 Statistical approach to investigating transport through single molecules *Phys. Rev. Lett.* **98** 176807
- [5] Hybertsen M S, Venkataraman L, Klare J E, Whalley A C, Steigerwald M L and Nuckolls C 2008 Amine-linked single-molecule circuits: systematic trends across molecular families *J. Phys.: Condens. Matter* **20** 374115
- [6] 2008 *Jaguar 7.5* Schrodinger, L.L.C., New York, NY
- [7] Kadantsev E S, Stott M J and Rubio A 2006 Electronic structure and excitations in oligoacenes from *ab initio* calculations *J. Chem. Phys.* **124** 134901
- [8] Kamenetska M, Koentopp M, Whalley A, Park Y S, Steigerwald M, Nuckolls C, Hybertsen M and Venkataraman L 2009 Formation and evolution of single-molecule junctions *Phys. Rev. Lett.* **102** 126803
- [9] Li Y W, Zhao J W, Yin X, Liu H M and Yin G P 2007 Conformational analysis of diphenylacetylene under the influence of an external electric field *Phys. Chem. Chem. Phys.* **9** 1186–93
- [10] Liang W J, Shores M P, Bockrath M, Long J R and Park H 2002 Kondo resonance in a single-molecule transistor *Nature* **417** 725–9
- [11] Martin C A, Ding D, van der Zant H S J and van Ruitenbeek J M 2008 Lithographic mechanical break junctions for single-molecule measurements in vacuum: possibilities and limitations *New J. Phys.* **10** 065008
- [12] Park J et al 2002 Coulomb blockade and the Kondo effect in single-atom transistors *Nature* **417** 722–5
- [13] Perdew J P, Burke K and Ernzerhof M 1996 Generalized gradient approximation made simple *Phys. Rev. Lett.* **77** 3865–8
- [14] Quek S Y, Choi H J, Louie S G and Neaton J B 2009 Length dependence of conductance in aromatic single-molecule junctions *Nano Lett. ASAP* doi:10.1021/ml9021336
- [15] Quek S Y, Venkataraman L, Choi H J, Louie S G, Hybertsen M S and Neaton J B 2007 Amine-gold linked single-molecule circuits: experiment and theory *Nano Lett.* **7** 3477–82
- [16] Reed M A, Zhou C, Muller C J, Burgin T P and Tour J M 1997 Conductance of a molecular junction *Science* **278** 252–4
- [17] Reichert J, Ochs R, Beckmann D, Weber H B, Mayor M and von Lohneysen H 2002 Driving current through single organic molecules *Phys. Rev. Lett.* **88** 176804
- [18] Venkataraman L, Klare J E, Tam I W, Nuckolls C, Hybertsen M S and Steigerwald M L 2006 Single-molecule circuits with well-defined molecular conductance *Nano Lett.* **6** 458–62
- [19] Venkataraman L, Park Y S, Whalley A C, Nuckolls C, Hybertsen M S and Steigerwald M L 2007 Electronics and chemistry: varying single molecule junction conductance using chemical substituents *Nano Lett.* **7** 502–6
- [20] Wu S M, Gonzalez M T, Huber R, Grunder S, Mayor M, Schonenberger C and Calame M 2008 Molecular junctions based on aromatic coupling *Nat. Nanotechnol.* **3** 569–74
- [21] Xu B Q and Tao N J J 2003 Measurement of single-molecule resistance by repeated formation of molecular junctions *Science* **301** 1221–3